



Application of a Hyperelastic 3D Printed Scaffold for Mesenchymal Stem Cell-Based Fabrication of a Bizonal Tendon Enthesis-like Construct

Riccardo Gottardi^{1,2,3*}, Kim Moeller², Roberto Di Gesù^{1,3}, Rocky S. Tuan^{2,4}, Martijn van Griensven⁵ and Elizabeth R. Balmayor⁶

¹Division of Pulmonary Medicine, Department of Pediatrics, Perelman School of Medicine, Department of Bioengineering, School of Engineering and Applied Science, University of Pennsylvania, Philadelphia, PA, United States, ²Center for Cellular and Molecular Engineering, Department of Orthopaedic Surgery, School of Medicine, University of Pittsburgh, Pittsburgh, PA, United States, ³Fondazione Ri.MED, Palermo, Italy, ⁴The Chinese University of Hong Kong, Hong Kong, China, ⁵Department cBITE, MERLN, Institute for Technology-Inspired Regenerative Medicine, Maastricht University, Maastricht, Netherlands, ⁶Department IBE, MERLN, Institute for Technology-Inspired Regenerative Medicine, Maastricht University, Maastricht, Netherlands

OPEN ACCESS

Edited by:

Michel Assad,
Charles River Laboratories

Reviewed by:

Cathy Melanie Tkaczyk,
Johnson and Johnson, France
Anik Chevrier,
École Polytechnique de Montréal,
Canada

*Correspondence:

Riccardo Gottardi
gottardir@email.chop.edu

Specialty section:

This article was submitted to
Biomaterials,
a section of the journal
Frontiers in Materials

Received: 01 October 2020

Accepted: 14 January 2021

Published: 08 March 2021

Citation:

Gottardi R, Moeller K, Di Gesù R,
Tuan RS, van Griensven M and
Balmayor ER (2021) Application of a
Hyperelastic 3D Printed Scaffold for
Mesenchymal Stem Cell-Based
Fabrication of a Bizonal Tendon
Enthesis-like Construct.
Front. Mater. 8:613212.
doi: 10.3389/fmats.2021.613212

After surgical tendon repair, the tendon-to-bone enthesis often does not regenerate, which leads to high numbers of rupture recurrences. To remedy this, tissue engineering techniques are being pursued to strengthen the interface and improve regeneration. In this study, we used hyperelastic biphasic 3D printed PLGA scaffolds with aligned pores at the tendon side and random pores at the bone side to mimic the native insertion side. In an attempt to recreate the enthesis, the scaffolds were seeded with adult human mesenchymal stem cells and then cultured in dual fluidic bioreactors, which allows the separate in-flow of tenogenic and chondrogenic differentiation media. MTS assay confirmed the ability of cells to proliferate in dual-flow bioreactors at similar levels to tissue culture plate. Hematoxylin-eosin staining confirmed a compact cell layer entrapped within newly deposited extracellular matrix attached to the scaffolds' fibers and between the porous cavities, that increased with culture time. After 7, 14, and 21 days, samples were collected and analyzed by qRT-PCR and GAG production. Cultured constructs in dual fluidic bioreactors differentiate regionally toward a tenogenic or chondrogenic fate dependent on exposure to the corresponding differentiation medium. SOX9 gene expression was upregulated (up to 50-fold compared to control) in both compartments, with a more marked upregulation in the cartilaginous portion of the scaffold. By day 21, the cartilage matrix marker, collagen II, and the tendon specific marker, tenomodulin, were found to be highly upregulated in the cartilaginous and tendinous portions of the construct, respectively. In addition, GAG production in the treated constructs (serum-free) matched that in control constructs exposed to 10% fetal bovine serum, confirming the support of functional matrix formation in this system. In summary, our findings have validated this dual fluidic system as a potential platform to form

the tendon enthesis, and will be optimized in future studies to achieve the fabrication of distinctly biphasic constructs.

Keywords: tendon, enthesis, bioreactor, hyperelastic, bioink, cartilage, bioprinting, tissue engineering

INTRODUCTION

The tendon-to-bone enthesis (TTBE) is a specialized connective tissue structure essential to guarantee a smooth transition between tendons and bones (Font Tellado et al., 2018). The main function of TTBE is to transfer forces from muscles to bones and to ensure joint stability during every day movements (Font Tellado et al., 2018). Thus, entheses are usually subjected to frequent and repeated tensile and compressive loading (Shaw and Benjamin, 2007), and this highly demanding environment calls for a strong structure able to withstand mechanical stress. Moving from muscle to bone, the TTBE composition gradually changes from aligned tendon fibers to unmineralized fibrocartilage, which becomes mineralized immediately before the bone insertion. The closer the tissue is to bone, the higher is the calcium content between collagen fibers, and the lower is fiber alignment (Font Tellado et al., 2017). The fibrocartilage layer is mainly composed of fibrochondrocytes entrapped in a matrix of collagen type II and aggrecan. This layer serves to ensure a gradual structural transition from tendon to bone (Moffat et al., 2008). Injuries affecting the TTBE have high clinical incidence especially in the elderly and in the more active populations that play sports, at both the professional and non-professional level. It is estimated that each year in the EU and the United States about 30 million people undergo tendon/ligament repair procedures, causing an annual expense of over €150 billion (Di Gesù et al., 2019). To date, surgical repair is the only treatment able to partially restore joint functionality after a TTBE injury. Despite several innovative techniques that have been developed (Rothrauff et al., 2020), surgical repair of massive enthesis injuries is still inadequate, with up to 79% failure rate in the most severe cases (Galatz et al., 2004; Mall et al., 2014; Henry et al., 2015). The main reason for failure is the poor healing properties of fibrocartilage in the native enthesis, which does not regenerate after surgical repair. Instead, collagen fibers of the tendon appear to directly insert into bone, and the mismatch in mechanical properties without a fibrocartilaginous transition layer predisposes to repair failure and recurrences (Thomopoulos et al., 2003). In principle, tissue engineering can significantly contribute to address these issues by actively promoting the recovery of a fibrocartilaginous layer. However, the realization of an engineered TTBE is particularly challenging due to the intrinsic complexity of the TTBE and the still limited understanding of its development (Spalazzi et al., 2006; Qu et al., 2015). Inspired by this challenging scenario, we hypothesized that a scaffold-based approach mimicking the structural features of the TTBE may be able also to support tissue regeneration and ultimately help in restoring TTBE functionality (Font Tellado et al., 2017). For this reason, in this work we describe the realization of a cellularized graft mimicking the tendon-fibrocartilaginous biphasic transition tissue of the TTBE. The construct is composed of a tendon-like side and a cartilage-like

side, cellularized with adult human mesenchymal stem cells (hMSCs). hMSCs represent a good choice to promote *de novo* regeneration, owing to their relative abundant availability and to their differentiation potential into all cellular phenotypes of the musculoskeletal lineage (Nancarrow-Lei et al., 2017). The structural core of our construct is a scaffold composed of medical-grade poly (L-lactide-co-glycolide) (PLGA), with high internal porosity and elastic properties sufficient to form a self-supporting mesh (Dewey et al., 2020), and able to support cell proliferation (Jakus et al., 2018). The pore architecture was specified for each tissue-type with changes in both dimension and distribution, smaller and aligned at the tendon side to favor the aligned deposition of collagen fibers, and larger and more randomly distributed at the cartilaginous side to mimic the architecture of cartilage.

For TTBE regeneration, hMSCs need to be differentiated toward a tenogenic and chondrogenic phenotype simultaneously within the scaffold. However, the induction of multiple specific phenotypes within a single construct is often challenging, as each specification process requires a different culture medium. Specifically, several studies have shown that serum free conditions enhance chondrogenesis (Valonen et al., 2010; Angelozzi et al., 2017), whereas the presence of serum is not detrimental in tenogenesis. Hence, the cell laden scaffold were maintained in culture within a dual flow biphasic bioreactor system we have previously established (Lin et al., 2014; Iannetti et al., 2016), which allows the feeding of two separate differentiation media simultaneously in different segments of the scaffold, thus enabling for bizonal differentiation of hMSCs. To assess stem cell differentiation toward a chondrogenic phenotype, we monitored the expression of the cartilage specific genes *SOX9* (Kim et al., 2019) and *COL2A1* (Lian et al., 2019), while for tenogenic differentiation we examined the expression of *TNMD*, which is a specific marker for tendon and ligaments (Shukunami et al., 2016).

MATERIALS AND METHODS

Cells

In this work, adult human bone marrow derived mesenchymal stem cells (hMSCs) were used. Cells were isolated from the femoral heads of 9 male donors (56–81 years old) undergoing total hip arthroplasty, a common and traditionally accessible source of bone marrow (Nöth et al., 2002; Song et al., 2005), with Institutional Review Board approval (University of Washington and University of Pittsburgh) following our standard protocol (Lin et al., 2014; Rothrauff et al., 2018). Briefly, trabecular bone was cored out using a curette, and put inside a Petri dish containing rinsing medium (RM: DMEM (Gibco, United States) supplemented with 1% v/v antibiotic-antimycotic

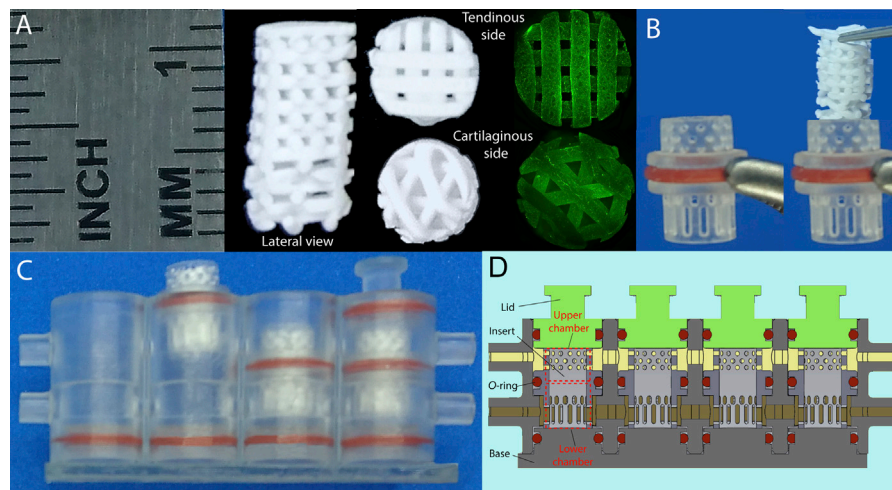


FIGURE 1 | (A) Macroscopic scaffolds appearance before cell seeding (white) and at day 7 after seeding (green fluorescence based on FITC-phalloidin staining, high resolution images available as SI, **Supplementary Figures S1, S2**). **(B)** scaffold placement within insert, and **(C)** phases of bioreactor assembly. **(D)** Schematic representation of a bioreactor compartment.

solution (Gibco, United States)). Trabecular bone was minced into small pieces to expose the bone marrow, and the suspension was then filtered through 40 μm filter to separate cells from bone chips. Finally, cells were resuspended with growth medium (GM: DMEM supplemented with 1% v/v antibiotic-antimycotic solution, and 10% v/v fetal bovine serum (Gibco, United States)) and passaged with GM. All experiments described in this work were conducted with cells at passage 3.

Cell Laden Scaffold Fabrication

Scaffolds were composed of medical-grade poly (L -lactide- co -glycolide) (PLGA) with $\geq 95\%$ internal porosity and hyperelastic properties (2.7 ± 0.8 MPa Elastic Modulus) commercialized as the Fluffy-X 3D-Printable Universal Scaffold system (Jakus et al., 2018) (**Figure 1A**). The material was provided by Dimension Inx (Dimension Inx, United States) having an open 0° – 90° pore pattern, and an interfiber distance of ~ 150 μm at the tendon side and of ~ 300 μm at the cartilage side. The material was provided as a square shaped sheet (thickness = 8 mm, height = 4 mm) from which cylinders were punched out using a 4 mm biopsy punch equipped with a plunger (Integra, United States).

The scaffolds were sterilized immediately before cell seeding by immersion in 70% v/v ethanol for 60 min under gentle agitation, followed by three washing cycles with sterile phosphate-buffered saline (PBS). Each scaffold was then grossly dried using a sterile wipe to remove excess PBS prior to cell seeding. hMSCs were randomly split into 3 different lots, each lot containing cells from 3 different donors ($n = 9$), and 4×10^5 cells/scaffold were seeded. The cell-laden scaffolds were then inserted in the bioreactor (**Figure 1B**) or cultured in a standard tissue culture plate (control).

FITC-Phalloidin Staining

Constructs were fixed for 2 h at room temperature using a 4% v/v paraformaldehyde/PBS solution (Thermo Scientific,

United States), rinsed thrice with fresh PBS and incubated with 0.1% v/v Triton-X (Sigma-Aldrich, United States)/PBS at room temperature for 10 min. Then, constructs were washed thrice with fresh PBS, incubated with 1% w/v Bovine Serum Albumin (BSA) (Sigma-Aldrich, United States)/PBS to saturate non-specific binding sites, washed thrice with fresh PBS and incubated with a 0.005% w/v FITC-Phalloidin (Sigma-Aldrich, United States)/1% BSA/PBS solution. The constructs were rinsed with PBS and stored at 4°C in dark condition until imaging with a Keyence BZX800 (Japan) microscope ($\lambda_{\text{Ex}} = 470/40$ nm, $\lambda_{\text{Em}} = 525/50$ nm).

Dual Fluidic Bioreactor

The bioreactor is composed of a body with cylindrical inner space that can be fed through an upper and a lower inlet. The body is isolated from the external environment by a base (on the bottom) and by four lids. Engineered constructs are placed within an inner insert, which has a hollow interior and includes a central protruding ring having an outer diameter approximating the inner diameter of the body. The insert is characterized by lateral perforations, which allow flow of medium through the tissue. Such insert divides the interior of the body into an upper chamber and a lower chamber so that fluids can flow through the insert perforations. All the connections between the body and the other components are equipped with silicone O-rings, which avoid liquid leaking during medium flow (Lozito et al., 2013; Alexander et al., 2014; Lin et al., 2014; Iannetti et al., 2016; Piroso et al., 2018).

Culturing and Differentiation Assay

The culture system was set to transfer media from the 20 ml reservoir syringes (BD, United States) to the collection 10 ml sterile bags (Kiyatec, United States) perfusing through the bioreactor at a constant flow of 0.083 ml/h (equivalent to ~ 2 ml/day).

Cell laden scaffolds were cultured in growth medium Colourless GM (CGM: FluoBrite (Gibco, United States) supplemented with 1% v/v Glutamax (Gibco, United States), 1% v/v sodium pyruvate (Gibco, United States), 1% v/v antibiotic-antimycotic solution (Gibco, United States), and 10% v/v fetal bovine serum (Gibco, United States)) for 7 days, with assays performed at days 1, 3, and 7 for cell viability and proliferation assays.

For differentiation, scaffolds were cultured with tenogenic medium delivered to the upper bioreactor chamber (TM: FluoBrite (Gibco, United States) supplemented with 1% v/v Glutamax (Gibco, United States), 1% v/v sodium pyruvate (Gibco, United States), 1% v/v antibiotic-antimycotic solution (Gibco, United States), 2% v/v fetal bovine serum (Gibco, United States), 1% Insulin-Transferrin-Selenium (Thermo scientific, United States), 1 ng/ml TGF- β 2 (Peprotech, United States)) (Font Tellado et al., 2015), and chondrogenic specific media in the lower chamber (CM: FluoBrite (Gibco, United States) supplemented with 1% v/v Glutamax (Gibco, United States), 1% v/v sodium pyruvate (Gibco, United States), 1% v/v antibiotic-antimycotic solution (Gibco, United States), 1% Insulin-Transferrin-Selenium (Thermo scientific, United States), 40 μ g/ml L-proline (Sigma, United States), 0.1 μ M Dexamethasone (Sigma, United States), 50 μ g/ml Sodium ascorbate (Sigma, United States), 10 ng/ml TGF- β 3 (Peprotech, United States)). The system was maintained in a humidified tissue culture incubator at 37°C, 5% CO₂ throughout each experiment. As controls, cell-laden scaffolds were cultured in a cell culture plate in growth medium (GM: DMEM high glucose (Gibco, United States), 1% v/v antibiotic-antimycotic solution (Gibco, United States), and 10% v/v fetal bovine serum (Gibco, United States)) renewing the medium every 2 days.

Viability and Proliferation Assays

Viability was assessed using the Live/Dead staining kit (Molecular Probes, United States) as per the manufacturer's protocol. Briefly, scaffolds were incubated with Calcein AM/Ethidium bromide solution (4 μ M/8 μ M) for 20 min at 37°C, then images were acquired using an upright fluorescence stereomicroscope (Olympus SZX16, Japan).

Proliferation was assessed by the quantitative MTS CellTiter 96[®] AQueos Non-Radioactive Cell Proliferation Assay (Promega, United States) that measures metabolic activity, according to the manufacturer's protocol. Briefly, cells laden scaffolds were incubated for 3 h at room temperature in an MTS/GM solution, then the amount of produced formazan was quantified by measuring absorbance at 490 nm with a plate reader (Sinergy HT, BioTek, United States). The results are reported as the mean of three separate measurements \pm SD.

Histology

At each time point, scaffolds were fixed overnight in 4% paraformaldehyde (PFA) at 4°C, washed in PBS, and dehydrated using progressive ethanol/water solution (25, 50, 70, 95, and 100%) and xylene before embedding in paraffin. The samples were sectioned at 5 μ m thickness using a HS325

TABLE 1 | Primer sequences used for qRT-PCR analyses.

Genes	Forward (5'--> 3')	Reverse (3'--> 5')
COL2A1	AACCAGATTGAGAGCATCCG	ACCTTCATGGCGTCCAAG
SOX9	GAGCCGAAAGCGGAGCTGGAA	ACAGTCGCCGCTCCAAGTG
S18	GTAACCCGTTGAACCCATT	CCATCCAATCGGTAGTAGCG
TNMD	TGTGGACTGGTGTGGTATCC	AGTGCCATTCGCTTCTGAA

Microtome (Microm, United States), and collected on Colorfrost Plus Microscope Slides (ThermoFisher Scientific, United States). Hematoxylin and eosin (H&E) staining was performed following the Harris Hematoxylin and Eosin protocol. Briefly, samples were de-paraffinized by soaking twice in HistoClear for 3 min and rehydrated by dipping in a descending series of ethanol/water solutions. Slides were sequentially stained with H&E, washed with running tap water, then mounted with a coverslip and limonene mount medium (Fisher Scientific, United States).

GAG/DNA Content Evaluation

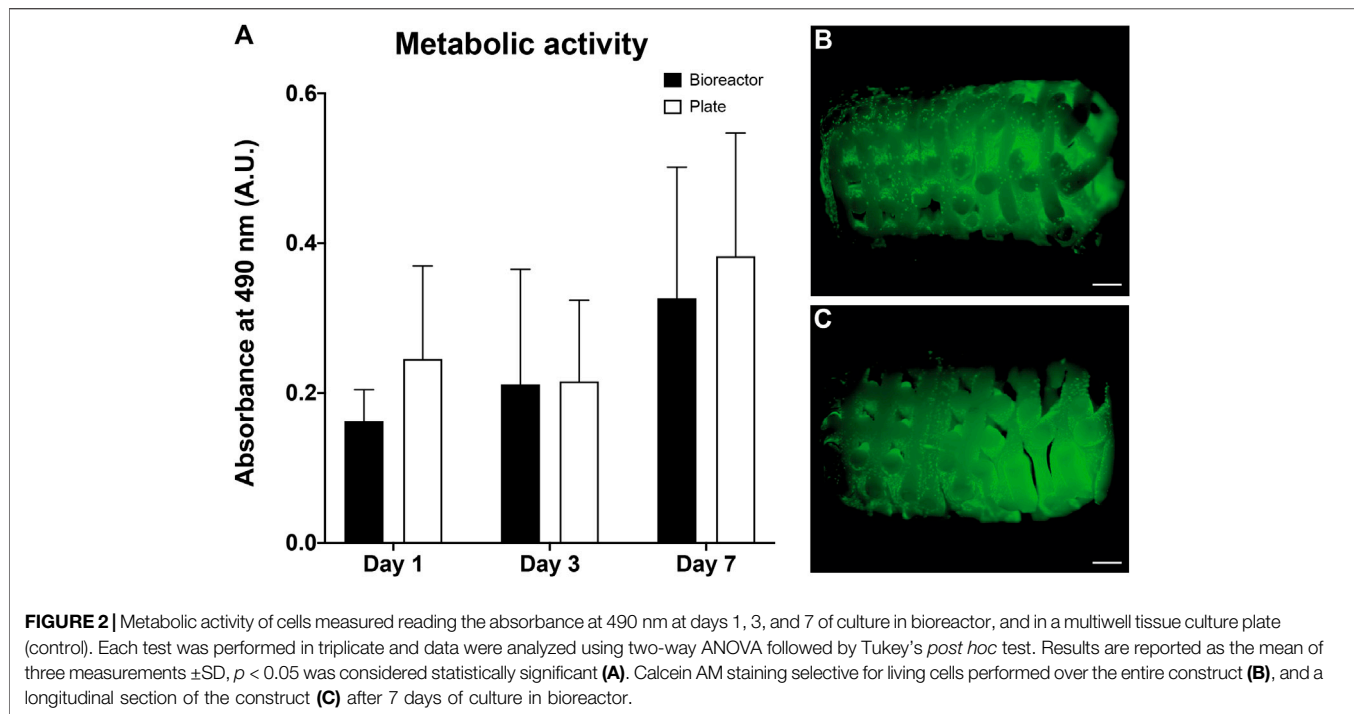
Sulfated GAG content was evaluated using the Bioscan Assay (Biocolor Ltd., United Kingdom) as per the manufacturer's instructions. Briefly, scaffolds were pre-digested with papain (Sigma-Aldrich, United States) for 3 h at 65°C. After incubation, the suspension was centrifuged, and the supernatant was collected and treated with Blyscan reagent for 30 min at room temperature. GAG content was quantified by measuring the absorbance at 656 nm with a plate reader. DNA content was quantified using the Picogreen assay (ThermoFisher, United States) according to the manufacturer's instructions. Briefly, samples were lyophilized, weighed, incubated with papain at 20 mg/ml, with 5 mM EDTA and 5 mM L-cysteine, at 60°C for 24 h. After incubation, samples were treated with Picogreen, and DNA was quantified by measuring the absorbance at 520 nm.

qRT-PCR

Scaffolds were flash frozen in liquid nitrogen and pulverized using a hammering set (Spectrum Bessmann, United States). RNA was extracted and isolated using the RNeasy Mini Kit according to the manufacturer's instructions (Qiagen, Germany). RNA was then converted to cDNA using the SuperScript IV First-Strand Synthesis System (Invitrogen, United States). Quantitative real-time PCR (qRT-PCR) was performed with a StepOne Plus Real-Time PCR system (Applied Biosystem, United States) using PowerUp SYBR Green Master Mix (Applied Biosystems, United States). The relative level of gene expression was calculated using the delta CT method. Gene primer sequences (Brand, Country) are shown in **Table 1**.

Statistical Analyses

Statistical analyses were performed using Prism 8 software version 8.2.1 (GraphPad software, United States) over four scaffold groups for each lot (pool of three donors). Metabolic activity and gene expression were analyzed using two-way ANOVA followed by Tukey's *post hoc* test. The GAG/DNA ratio was analyzed using an unpaired *t* test with Welch's



corrections. All data are expressed as means \pm standard deviation, and a p value of 0.05 was considered significant for all experiments.

RESULTS

Culturing in the Bioreactor Supports Cell Proliferation and Viability

Cell proliferation within the scaffold was evaluated using the MTS assay in constructs cultured either in a culture plate or within the dual fluidic (biphasic) bioreactor, with the same medium composition. Cell proliferative activity observed at days 1, 3, and 7 was comparable in both conditions at each time point, increasing as a function of time as expected for proliferating cells (**Figure 2A**). Such trend was more linear for constructs cultured within the dual fluidic bioreactor. Cell viability was confirmed at day 7 by incubation with Calcein AM, to fluorescently label (green) viable, metabolically active cells. Green-labeled cells were found to be uniformly distributed on the scaffold surface (**Figure 2B**) and within the scaffold as evidenced by imaging along a longitudinal section of the construct (**Figure 2C**).

3D Dynamic Culturing Promotes hMSCs Differentiation and ECM Production

To confirm hMSC differentiation into tenocyte and chondrocyte lineage, we analyzed the expression of tissue specific genes (*SOX9*, *COL2A1*, *TNMD*) in the cartilaginous and tendinous components of the constructs after culturing within the dual fluidic bioreactor. The expression of *SOX9* increased at day 7 in both construct

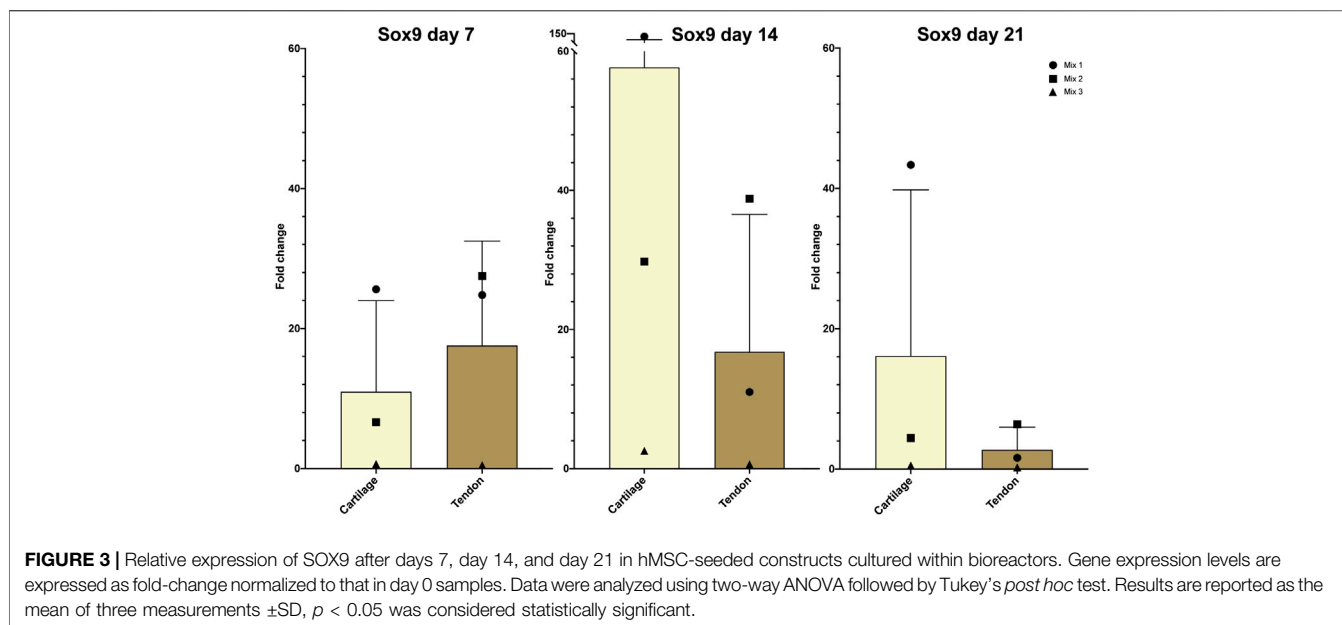
components (up to 50-folds change compared to day 0), and continued increasing in the whole scaffold up to day 14. Interestingly, *SOX9* expression maintained high values but started to decrease at day 21, with a more evident decrease in the tendinous component (**Figure 3**).

The histological morphology of the engineered constructs after culturing in the bioreactor was carried out with H&E staining at early (7 days) and late (21 days) time points. Large cell clusters were observed adherent to the surface of the scaffold. At day 7, such structures appeared as a thin monocellular layer (**Figures 4A,B**), and by day 21 these developed into thicker cell aggregates (**Figures 4C,D**) embedded in newly produced extracellular matrix (ECM). Results from GAG assay confirmed that the constructs cultured in the bioreactor in serum-free conditions produced significant amounts of GAG compared to the controls cultured in a tissue culture plate supplemented with 10% FBS (**Figure 4E**).

Furthermore, by day 21, the cartilage specific *COL2A1* gene and the tendon specific *TNMD* gene were highly expressed in the cartilaginous and tendinous components, respectively, when compared to the control at the same time point (**Figures 4F,G**). Taken together, these results further suggested tissue-specific differentiation toward chondrocyte and tenocyte lineages in the engineered constructs.

DISCUSSION

In this work, we have described the realization of an engineered biphasic construct with spatially distinct cartilaginous and tendinous components, supporting the feasibility of tissue engineering the tendon-to-bone entheses.



The structural core of our construct is a scaffold composed of medical-grade PLGA, with high internal porosity and elastic properties sufficient to form a self-supporting mesh (Dewey et al., 2020), and able to support cell viability and proliferation (Jakus et al., 2018). Furthermore, the scaffold has been previously reported to be cytocompatible and supportive of MSCs differentiation both *in vitro* and in mouse and macaque *in vivo* models (Jakus et al., 2016). The pore architecture varied in dimension and distribution, smaller and aligned on one side to mimic the physiologic alignment of tendon fibers, and larger and more randomly distributed on the other side to mimic the less ordered architecture of the cartilage matrix.

The scaffolds were cellularized using hMSCs, which are characterized by a high differentiation potential toward musculoskeletal lineages (Yang et al., 2013; Nancarrow-Lei et al., 2017; Iseki et al., 2019). Following this rationale, we chose to harvest cells from the femoral heads, which is characterized by a high content of bone marrow, which is rich in MSCs. Moreover, femoral heads are an easily accessible source from surgical waste following total hip arthroplasty. Cell laden scaffolds were cultured within our advanced biphasic bioreactor culture system, which is designed to host 3D engineered constructs or even native tissues and to provide two tissue-specific differentiation media, separately and simultaneously, without mixing (Iannetti et al., 2016). The main functional unit of this bioreactor is a dual flow 3D printed chamber (Figures 1A–C), extensively described in our previous work (Chiesa et al., 2021; Lozito et al., 2013; Alexander et al., 2014; Lin et al., 2014; Iannetti et al., 2016; Piroso et al., 2018, Piroso et al., 2020). The overall system is composed of an infusion pump, a medium reservoir(s), the bioreactor, and a collection bag. The bioreactor is a 3D printed array (Tuan et al., 2016) composed of four communicating compartments connected in series. Each compartment is divided into two chambers (upper and lower), which can be simultaneously fed with separate, specific culture

medium. The cell-seeded scaffolds are sized to fit inside an insert, which is placed within each compartment. The four compartments are isolated from the external environment by a base (bottom) and four lids (top), both equipped with silicon O-rings for sealing. As controls, we cultured cellularized scaffolds in growth medium in a tissue culture plate for simplicity of execution, since, in our hands, when a common medium is utilized the very slow flow rate in the bioreactor (~ 2 ml/day) is equivalent to the periodic medium change in a tissue culture plate and does not affect cell growth.

The setup of the biphasic culture systems allowed the delivery of separate teno- and chondrogenic media to the upper and lower chamber, respectively. Moreover, the flow rate was sufficient to guarantee oxygen and nutrient distribution while avoiding any mechanical stress to the cells. The efficacy of our system is confirmed by the MTS assay, which shows that cellular metabolic activity levels after 1, 3, and 7 days of culture in the biphasic bioreactor were comparable to those in constructs maintained in standard tissue culture plate culture at each of the corresponding time points (Figure 2A). These observations are further supported by the cell viability assays after 7 days of biphasic culturing. Fluorescence images show a homogeneous distribution of viable cells located on the surface (Figure 2B) as well as within the inner pores (Figure 2C) of the scaffold.

After assessing cell viability and proliferation, we administered selective differentiation stimuli to the construct, feeding tenogenesis and chondrogenesis specific media to the upper and lower chamber, respectively. We then confirmed teno- and chondrogenic specific lineage differentiation of the hMSCs by assessing the expression of tendon and cartilage specific genes (*SOX9*, *COL2A1*, *TNMD*) in the cartilaginous and tendinous components of the construct at each time point.

The expression of *SOX9* increased at day 7 in both components (up to 50-fold change compared to day 0), and remained elevated at day 14 (Figure 3). By day 21, *SOX9*

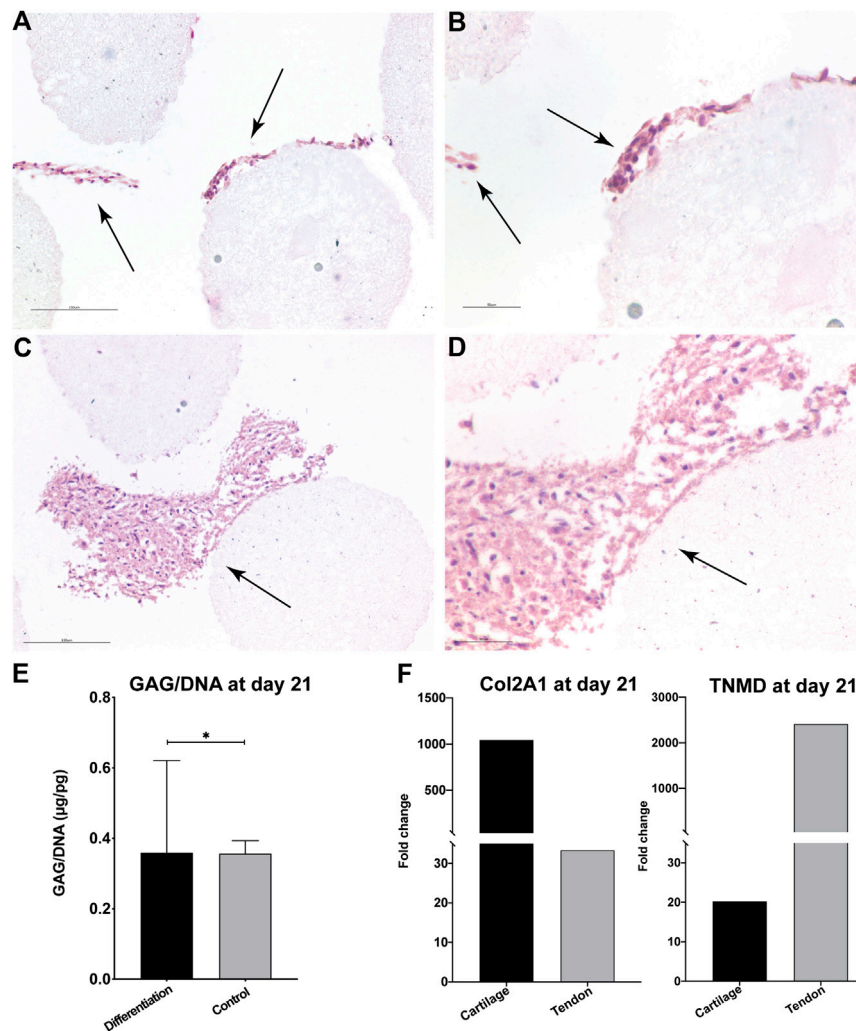


FIGURE 4 | H&E staining of the biphasic construct (cartilaginous side) after 7 days (**A, B**) and 21 days (**C, D**) of culture at two different magnifications. Black arrows indicate newly produced extracellular matrix. Scale bar = 150 µm (**A, C**) and 50 µm (**B, D**). Overview images of the whole construct are reported in **Supplementary Figure S3** (control) and **Supplementary Figure S4** (differentiated). GAG content of the constructs expressed as GAG/DNA ratio at day 21. Data were analyzed using an unpaired *t* test with Welch's corrections, **p* < 0.05 (**E**). Relative gene expression of COL2A1, and TNMD at day 21 measured by qRT-PCR (**F**) normalized to control at the same time point.

expression remained stable in the cartilaginous component, but had decreased in the tendinous component. The decreasing trend suggests a spatially specific differentiation of hMSCs into chondrocytes and tenocytes. Indeed, *SOX9* overexpression is specifically associated with chondrogenesis, acting to promote collagen type II expression and deposition (Ikeda et al., 2004), and inhibiting the synthesis of collagen type X (Leung et al., 2011). Interestingly, recent embryonic development studies have reported that *SOX9* is also essential for progenitor cells to differentiate into tenocytes (Sugimoto et al., 2012). In fact, consistent with our findings, Nagakura et al. (Nagakura et al., 2020) showed that murine tenoprogenitor cells transiently express *SOX9* in during development, and downregulate the same gene after differentiation to tenocytes *in vivo*.

These gene expression results are further supported by our histological findings. H&E staining highlighted cellular aggregates

attached onto scaffold fibers throughout the thickness of the construct, and matrix deposition appeared abundant. Remarkably, between day 7 (**Figures 4A,B**) and day 21 (**Figures 4C,D**), there was a significant increase in matrix deposition, and by the culture endpoint cells appeared to be integrated in a newly deposited ECM. Data from biochemical analysis of the constructors cultured in the biphasic bioreactor showed significantly increased in the GAG/DNA ratio, compared to control sample at the same time point. Moreover, additional qRT-PCR analyses of the chondrogenesis specific gene *COL2A1* and the tenogenesis specific gene *TNMD* further support the evidence of tissue specific differentiation. While *COL2A1* was highly overexpressed (1,000-fold change) in the cartilaginous side, *TNMD* was markedly overexpressed on the tendon side. Taken together, these results suggest a likely selective bizonal differentiation of hMSCs toward chondrogenic and tenogenic phenotypes within the hMSC-seeded biphasic scaffolds.

CONCLUSION

In this study, we have realized an engineered construct that recapitulates some aspects of the tendon-fibrocartilage transition tissue of a tendon-to-bone enthesis, and that can support cell viability, proliferation, and differentiation. Our differentiation system was based on a 3D printed, highly biocompatible scaffold of hyperelastic PLGA, characterized by a microporous architecture with aligned fiber orientation on the tendon side, and dishomogeneous fiber organization on the cartilaginous side, mimicking some anatomical features of the native enthesis.

Cellularized with hMSCs, the scaffolds were cultured within an advanced biphasic bioreactor system that allowed simultaneous exposure of each side of the biphasic construct to a specific differentiation medium. Results from gene expression analysis, biochemical analysis, and histological examination suggest that we have successfully obtained an engineered construct composed of a tendon-like side and a cartilage like side, that is potentially applicable for the surgical tendon repair after mechanical stimulation to assess resistance to tensile stress, an essential parameter to proceed to *in vivo* models.

DATA AVAILABILITY STATEMENT

The original contributions presented in the study are included in the article/**Supplementary Material**, further inquiries can be directed to the corresponding author.

ETHICS STATEMENT

The studies involving human participants were reviewed and approved by the IRB of the University of Washington and University of Pittsburgh. Written informed consent for participation was not required for this study in accordance

REFERENCES

- Alexander, P. G., Gottardi, R., Lin, H., Lozito, T. P., and Tuan, R. S. (2014). Three-dimensional osteogenic and chondrogenic systems to model osteochondral physiology and degenerative joint diseases. *Exp. Biol. Med.* 239 (9), 1080–1095. doi:10.1177/1535370214539232
- Angelozzi, M., Penolazzi, L., Mazzitelli, S., Lambertini, E., Lolli, A., Piva, R., et al. (2017). Dedifferentiated chondrocyte in composite microfibers as tool for cartilage repair. *Front. Bioeng. Biotechnol.* 5, 35. doi:10.3389/fbioe.2017.00035
- Chiesa, I., Di Gesù, R., Overholt, K. J., and Gottardi, R. (2021). "A mesoscale 3D culture system for native and engineered biphasic tissues: application to the osteochondral unit," in *Methods in molecular biology: organ-on-chip*.
- Dewey, M. J., Nosatov, A. V., Subedi, K., Shah, R., and Jakus, A. (2020). Inclusion of a 3D-printed Hyperelastic bone mesh improves mechanical and osteogenic performance of a mineralized collagen scaffold. *Acta Biomater.* 121, 224–236. doi:10.1016/j.actbio.2020.11.028
- Di Gesù, R., Amato, G., and Gottardi, R. (2019). Electrospun scaffolds in tendons regeneration: a review. *Muscle Ligaments Tendons J.* 9 (4), 478–493. doi:10.32098/mltj.04.2019.02
- Font Tellado, S., Balmayor, E. R., and Van Griensven, M. (2015). Strategies to engineer tendon/ligament-to-bone interface: Biomaterials, cells and growth factors. *Adv. Drug Delivery Rev.* 94, 126–140. doi:10.1016/j.addr.2015.03.004

with the national legislation and the institutional requirements.

AUTHOR CONTRIBUTIONS

RG and RDG performed the data analysis, statistical treatment, and with RT drafted the manuscript. KM and RDG performed all the experiments and acquired the data. RT provided support, cells, and instrumentation for the study and help supervise the experiments with RG. RG, MG, and EB designed the experiments and directed the study. MG and EB critically revised the manuscript.

FUNDING

This work is supported, in part, by the US Department of Defense (W81XWH-14-2-0003 to RST), by the EU Horizon 2020—Research and Innovation Action SC1-PM 17—2017 + Project OACTIVE (under Grant Agreement No. 777159 to RG), by Fondazione Ri.MED (to RG and RDG), and by the Children's Hospital of Philadelphia Research Institute (to RG).

ACKNOWLEDGMENTS

The authors would like to thank Paul Manner, University of Washington, for providing clinical specimens.

SUPPLEMENTARY MATERIAL

The Supplementary Material for this article can be found online at: <https://www.frontiersin.org/articles/10.3389/fmats.2021.613212/full#supplementary-material>.

- Font Tellado, S., Bonani, W., Balmayor, E. R., Foehr, P., Motta, A., Migliaresi, C., et al. (2017). Fabrication and characterization of biphasic silk fibroin scaffolds for tendon/ligament-to-bone tissue engineering. *Tissue Eng. Part A.* 23 (15-16), 859–872. doi:10.1089/ten.tea.2016.0460
- Font Tellado, S., Chiera, S., Bonani, W., Poh, P. S. P., Migliaresi, C., Motta, A., et al. (2018). Heparin functionalization increases retention of TGF- β 2 and GDF5 on biphasic silk fibroin scaffolds for tendon/ligament-to-bone tissue engineering. *Acta Biomater.* 72, 150–166. doi:10.1016/j.actbio.2018.03.017
- Galatz, L. M., Ball, C. M., Teefey, S. A., Middleton, W. D., and Yamaguchi, K. (2004). The outcome and repair integrity of completely arthroscopically repaired large and massive rotator cuff tears. *J. Bone Jt. Surg. Ser. A.* 86 (2), 219–224. doi:10.2106/00004623-200402000-00002
- Henry, P., Wasserstein, D., Park, S., Dwyer, T., Chahal, J., Slobogean, G., et al. (2015). Arthroscopic repair for chronic massive rotator cuff tears: a systematic review. *Arthroscopy. J. Arthroscopy Relat. Surg.* 31 (12), 2472–2480. doi:10.1016/j.arthro.2015.06.038
- Iannetti, L., Urso, G. D., Conoscenti, G., Cutri, E., Raimondi, M. T., Gottardi, R., et al. (2016). Distributed and lumped parameter models for the characterization of high throughput bioreactors. *PLoS One* 11 (9), e0162774. doi:10.1371/journal.pone.0162774
- Ikeda, T., Kamekura, S., Mabuchi, A., Kou, I., Seki, S., Takato, T., et al. (2004). The combination of SOX5, SOX6, and SOX9 (the SOX trio) provides signals

- sufficient for induction of permanent cartilage. *Arthritis Rheum.* 50 (11), 3561–3573. doi:10.1002/art.20611
- Iseki, T., Rothrauff, B. B., Kihara, S., Sasaki, H., Yoshiya, S., Fu, F. H., et al. (2019). Dynamic compressive loading improves cartilage repair in an in vitro model of microfracture: comparison of 2 mechanical loading regimens on simulated microfracture based on fibrin gel scaffolds encapsulating connective tissue progenitor cells. *Am. J. Sports Med.* 47 (9), 2188–2199. doi:10.1177/0363546519855645
- Jakus, A. E., Rutz, A. L., Jordan, S. W., Kannan, A., Mitchell, S. M., Yun, C., et al. (2016). Hyperelastic “bone”: a highly versatile, growth factor-free, osteoregenerative, scalable, and surgically friendly biomaterial. *Sci. Transl. Med.* 8 (358), 358ra127. doi:10.1126/scitranslmed.aaf7704
- Jakus, A. E., Geisendorfer, N. R., Lewis, P. L., and Shah, R. N. (2018). 3D-printing porosity: a new approach to creating elevated porosity materials and structures. *Acta Biomater.* 72, 94–109. doi:10.1016/j.actbio.2018.03.039
- Kim, S., Han, S., Kim, Y., Kim, H. S., Gu, Y. R., Kang, D., et al. (2019). Tankyrase inhibition preserves osteoarthritic cartilage by coordinating cartilage matrix anabolism via effects on SOX9 PARylation. *Nat. Commun.* 10 (1), 4898. doi:10.1038/s41467-019-12910-2
- Leung, V. Y. L., Gao, B., Leung, K. K. H., Melhado, I. G., Wynn, S. L., Au, T. Y. K., et al. (2011). SOX9 governs differentiation stage-specific gene expression in growth plate chondrocytes via direct concomitant transactivation and repression. *PLoS Genet.* 7 (11), e1002356. doi:10.1371/journal.pgen.1002356
- Lian, C., Wang, X., Qiu, X., Wu, Z., Gao, B., Liu, L., et al. (2019). Collagen type II suppresses articular chondrocyte hypertrophy and osteoarthritis progression by promoting integrin β 1–SMAD1 interaction. *Bone Res.* 7 (1), 8. doi:10.1038/s41413-019-0046-y
- Lin, H., Lozito, T. P., Alexander, P. G., Gottardi, R., and Tuan, R. S. (2014). Stem cell-based microphysiological osteochondral system to model tissue response to interleukin-1B. *Mol. Pharm.* 11 (7), 2203–2212. doi:10.1021/mp500136b
- Lozito, T. P., Alexander, P. G., Gottardi, R., Cheng Wai-Ming, A., and Tuan, R. S. (2013). Three-dimensional osteochondral microtissue to model pathogenesis of osteoarthritis. *Stem Cell Res. Ther.* 4 (Suppl 1), S6. doi:10.1186/srct367
- Mall, N. A., Tanaka, M. J., Choi, L. S., and Paletta, G. A. (2014). Factors affecting rotator cuff healing. *J. Bone Jt. Surg.* 96 (9), 778–788. doi:10.2106/JBJS.M.00583
- Moffat, K. L., Sun, W. H. S., Pena, P. E., Chahine, N. O., Doty, S. B., Ateshian, G. A., et al. (2008). Characterization of the structure-function relationship at the ligament-to-bone interface. *Proc. Natl. Acad. Sci. U.S.A.* 105 (23), 7947–7952. doi:10.1073/pnas.0712150105
- Nagakura, R., Yamamoto, M., Jeong, J., Hinata, N., Katori, Y., Chang, W. J., et al. (2020). Switching of Sox9 expression during musculoskeletal system development. *Sci. Rep.* 10 (1), 1–12. doi:10.1038/s41598-020-65339-9
- Nancarrow-Lei, R., Mafi, P., Mafi, R., and Khan, W. (2017). A systemic review of adult mesenchymal stem cell sources and their multilineage differentiation potential relevant to musculoskeletal tissue repair and regeneration. *Curr. Stem Cell Res. Ther.* 12 (8), 601–610. doi:10.1155/2020/4173578
- Nöth, U., Tuli, R., Osyczka, A. M., Danielson, K. G., and Tuan, R. S. (2002). In vitro engineered cartilage constructs produced by press-coating biodegradable polymer with human mesenchymal stem cells. *Tissue Eng.* 8 (1), 131–144. doi:10.1089/107632702753503126
- Pirosa, A., Gottardi, R., Alexander, P. G., and Tuan, R. S. (2018). Engineering in-vitro stem cell-based vascularized bone models for drug screening and predictive toxicology. *Stem Cell Res. Ther.* 9 (1), 112. doi:10.1186/s13287-018-0847-8
- Pirosa, A., Gottardi, R., Alexander, P. G., Puppi, D., Chiellini, F., and Tuan, R. S. (2020). An in vitro chondro-osteo-vascular triphasic model of the osteochondral complex. Available at: <https://t.co/hrUu3i6K1Y> (Accessed August 27, 2020).
- Qu, D., Mosher, C. Z., Boushell, M. K., and Lu, H. H. (2015). Engineering complex orthopaedic tissues via strategic biomimicry. *Ann. Biomed. Eng.* 43 (3), 697–717. doi:10.1007/s10439-014-1190-6
- Rothrauff, B. B., Coluccino, L., Gottardi, R., Ceseracciu, L., Scaglione, S., Goldoni, L., et al. (2018). Efficacy of thermoresponsive, photocrosslinkable hydrogels derived from decellularized tendon and cartilage extracellular matrix for cartilage tissue engineering. *J. Tissue Eng. Regen. Med.* 12 (1), e159–e170. doi:10.1002/term.2465.Efficacy
- Rothrauff, B. B., Jorge, A., de Sa, D., Kay, J., Fu, F. H., and Musahl, V. (2020). Anatomic ACL reconstruction reduces risk of post-traumatic osteoarthritis: a systematic review with minimum 10-year follow-up. *Knee Surg. Sports Traumatol. Arthrosc.* 28 (4), 1072–1084. doi:10.1007/s00167-019-05665-2
- Shaw, H. M., and Benjamin, M. (2007). Structure-function relationships of entheses in relation to mechanical load and exercise. *Scand. J. Med. Sci. Sports* 17 (4), 303–315. doi:10.1111/j.1600-0838.2007.00689.x
- Shukunami, C., Yoshimoto, Y., Takimoto, A., Yamashita, H., and Hiraki, Y. (2016). Molecular characterization and function of tenomodulin, a marker of tendons and ligaments that integrate musculoskeletal components. *Jpn. Dent. Sci. Rev.* 52 (4), 84–92. doi:10.1016/j.jdsr.2016.04.003
- Song, L., Young, N. J., Webb, N. E., and Tuan, R. S. (2005). Origin and characterization of multipotential mesenchymal stem cells derived from adult human trabecular bone. *Stem Cell Dev.* 14 (6), 712–721. doi:10.1089/scd.2005.14.712
- Spalazzi, J. P., Doty, S. B., Moffat, K. L., Levine, W. N., and Lu, H. H. (2006). Development of controlled matrix heterogeneity on a triphasic scaffold for orthopedic interface tissue engineering. *Tissue Eng.* 12 (12), 3497–3508. doi:10.1089/ten.2006.12.3497
- Sugimoto, Y., Takimoto, A., Akiyama, H., Kist, R., Scherer, G., Nakamura, T., et al. (2012). Scx+/Scx9+ progenitors contribute to the establishment of the junction between cartilage and tendon/ligament. *Development* 140 (11), 2280–2288. doi:10.1242/dev.096354
- Thomopoulos, S., Williams, G. R., and Soslowsky, L. J. (2003). Tendon to bone healing: differences in biomechanical, structural, and compositional properties due to a range of activity levels. *J. Biomech. Eng.* 125 (1), 106–113. doi:10.1115/1.1536660
- Tuan, R. S., Lin, H., Lozito, T. P., Alexander, P., Douglas, A. N. J., and Gottardi, R. (2016). Patent application publication. Pub. No.: US 2016/0271610 A1, 1, 1–5.
- Valonen, P. K., Moutos, F. T., Kusanagi, A., Moretti, M., Diekmann, B. O., Welter, J. F., et al. (2010). In vitro generation of mechanically functional cartilage grafts based on adult human stem cells and 3D-woven poly(ϵ -caprolactone) scaffolds. *Biomaterials* 31 (8), 2193–2200. doi:10.1016/j.biomaterials.2009.11.092
- Yang, G., Rothrauff, B. B., Lin, H., Gottardi, R., Alexander, P. G., and Tuan, R. S. (2013). Enhancement of tenogenic differentiation of human adipose stem cells by tendon-derived extracellular matrix. *Biomaterials* 34 (37), 9295–9306. doi:10.1038/jid.2014.371

Conflict of Interest: The authors declare that the research was conducted in the absence of any commercial or financial relationships that could be construed as a potential conflict of interest.

Copyright © 2021 Gottardi, Moeller, Di Gesù, Tuan, van Griensven and Balmayor. This is an open-access article distributed under the terms of the Creative Commons Attribution License (CC BY). The use, distribution or reproduction in other forums is permitted, provided the original author(s) and the copyright owner(s) are credited and that the original publication in this journal is cited, in accordance with accepted academic practice. No use, distribution or reproduction is permitted which does not comply with these terms.